Article

Long-Living Intermediates during a Lamellar to a Diamond-Cubic Lipid Phase Transition: A Small-Angle X-Ray Scattering Investigation

Borislav Angelov, Angelina Angelova, Ulla Vainio, Vasil M. Garamus, Sylviane Lesieur, Regine Willumeit, and Patrick Couvreur

Langmuir, **2009**, 25 (6), 3734-3742• DOI: 10.1021/la804225j • Publication Date (Web): 17 February 2009

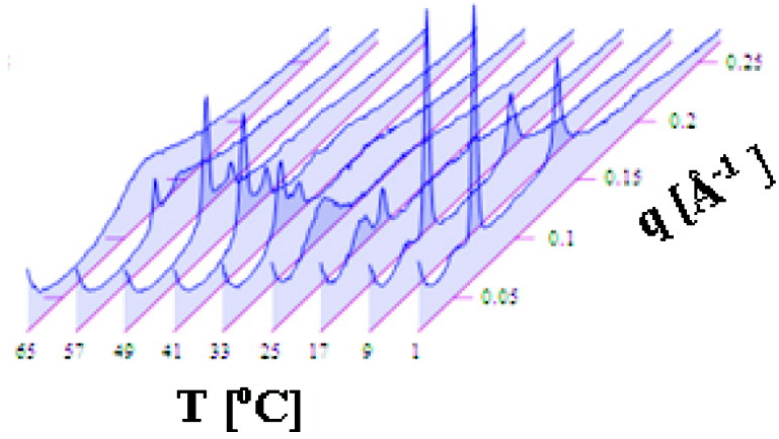

More About This Article

Additional resources and features associated with this article are available within the HTML version:

- Supporting Information
- Access to high resolution figures
- Links to articles and content related to this article
- Copyright permission to reproduce figures and/or text from this article

View the Full Text HTML

Long-Living Intermediates during a Lamellar to a Diamond-Cubic Lipid Phase Transition: A Small-Angle X-Ray Scattering Investigation

Borislav Angelov,[†,||] Angelina Angelova,*[,‡,§] Ulla Vainio,[⊥] Vasil M. Garamus,[||] Sylviane Lesieur,[‡,§] Regine Willumeit,[||] and Patrick Couvreur[‡,§]

Institute of Biophysics, Bulgarian Academy of Sciences, BG-1113 Sofia, Bulgaria, CNRS UMR8612 Physico-chimie-Pharmacotechnie-Biopharmacie, Châtenay-Malabry, F-92296 France, University Paris Sud, Châtenay-Malabry, F-92296 France, Institute of Materials Research, GKSS Research Center, Geesthacht, D-21502 Germany, and HASYLAB c/o DESY, Notkestrasse 85, Hamburg, D-22603 Germany

Received May 19, 2008

To generate nanostructured vehicles with tunable internal organization, the structural phase behavior of a self-assembled amphiphilic mixture involving poly(ethylene glycol) monooleate (MO-PEG) and glycerol monooleate (MO) is studied in excess aqueous medium by time-resolved small-angle X-ray scattering (SAXS) in the temperature range from 1 to 68 °C. The SAXS data indicate miscibility of the two components in lamellar and nonlamellar soft-matter nanostructures. The functionalization of the MO assemblies by a MO-PEG amphiphile, which has a flexible large hydrophilic moiety, appears to hinder the epitaxial growth of a double diamond (D) cubic lattice from the lamellar (L) bilayer structure during the thermal phase transition. The incorporated MO-PEG additive is found to facilitate the formation of structural intermediates. They exhibit greater characteristic spacings and large diffusive scattering in broad temperature and time intervals. Their features are compared with those of swollen long-living intermediates in MO/octylglucoside assemblies. A conclusion can be drawn that long-living intermediate states can be equilibrium stabilized in two- or multicomponent amphiphilic systems. Their role as cubic phase precursors is to smooth the structural distortions arising from curvature mismatch between flat and curved regions. The considered MO-PEG functionalized assemblies may be useful for preparation of sterically stabilized liquid-crystalline nanovehicles for confinement of therapeutic biomolecules.

Introduction

Functional soft-matter nanostructured materials are frequently self-assembled with multicomponent amphiphilic compositions.[1−7] The generation of hierarchically organized amphiphile-based systems requires methodological advancements toward creation of nanoperiodic templates with complex geometries.[8−12] The controlled nanocompartmentalization and functionalization of lipid liquid crystalline assemblies represent some of the forefront approaches.[13−17] Nanoscale lipid-based drug delivery and diagnostic systems for biomedical applications often involve additives such as polyethylene glycol (PEG) amphiphile derivatives and nonionic detergents displaying dispersion and noncytotoxic properties.[18,19]

Structural investigations of the dynamics of the topological transitions in such amphiphilic materials will have an impact on the development of new nanocarrier and diagnostic assemblies in addition to their broad applications as templates for synthesis

* Corresponding author. E-mail: angelina.angelova@u-psud.fr.
† Bulgarian Academy of Sciences.
‡ CNRS UMR8612 Physico-chimie-Pharmacotechnie-Biopharmacie.
§ University Paris Sud.
|| Institute of Materials Research.
⊥ HASYLAB c/o DESY.

(1) Moitzi, C.; Guillot, S.; Fritz, G.; Salentinig, S.; Glatter, O. *Adv. Mater.* **2007**, *19*, 1352.
(2) (a) Mezzenga, R.; Schurtenberger, P.; Burbidge, A.; Michel, M. *Nat. Mater.* **2005**, *4*, 729. (b) Mezzenga, R.; Meyr, C.; Servais, C.; Romoscanu, A. I.; Sagalowicz, L.; Hayward, R. C. *Langmuir* **2005**, *21*, 3322.
(3) (a) Gerard, C. L.; Wong, J. X. T.; Alison, L.; Youli, L.; Janmey, P. A.; Safinya, C. R. *Science* **2000**, *288*, 2035. (b) Lei, N.; Safinya, C. R.; Roux, D.; Liang, K. S. *Phys. Rev. E* **1997**, *56*, 608.
(4) Ghoroghchian, P.; Frail, P. R.; Susumu, K.; Blessington, D.; Brannan, A. K.; Bates, F. S.; Chance, B.; Hammer, D. A.; Therien, M., J. *Proc. Natl. Acad. Sci. U.S.A.* **2005**, *102*, 2922.
(5) Teixeira, H.; Dubernet, C.; Rosilio, V.; Benita, S.; Lepault, J.; Erk, I.; Couvreur, P. *Pharm. Res.* **2000**, *17*, 1329.
(6) (a) Angelova, A.; Ollivon, M.; Campitelli, A.; Bourgaux, C. *Langmuir* **2003**, *19*, 6928. (b) Angelova, A.; Angelov, B.; Papahadjopoulos-Sternberg, B.; Ollivon, M.; Bourgaux, C. *J. Drug Delivery Sci. Technol.* **2005**, *15*, 108. (c) Angelova, A.; Angelov, B.; Papahadjopoulos-Sternberg, B.; Bourgaux, C.; Couvreur, P. *J. Phys. Chem. B* **2005**, *109*, 3089.
(7) Case, F.; Alexandridis, P., Eds. *Mesoscale Phenomena in Fluid Systems*; ACS Symp.Series 861, American Chemical Society: Washington DC, 2003.
(8) Lynch, M. L.; Spicer P. T., Eds. *Bicontinuous Liquid Crystals*; (Surfactant Science Series), Taylor & Francis: Boca Raton, 2005; Vol. 127.
(9) Hyde, S.; Andersson, S.; Larsson, K.; Blum, Z.; Landh, T.; Lidin, S.; Ninham, B. W. *The Language of Shape*; Elsevier Science: New York, 1996.
(10) (a) Hyde, S. T.; Schroder, G. E. *Curr. Opin. Colloid Interface Sci.* **2003**, *8*, 5. (b) Hyde, S. T. *Colloid Surf. A* **1997**, *129*, 207. (c) Andersson, S.; Hyde, S. T.; Larsson, K.; Lidin, S. *Chem. Rev.* **1988**, *88*, 221.
(11) (a) Piotto, S. *Origins Life Evol. Biosphere* **2004**, *34*, 123. (b) Shearman, G. C.; Ces, O.; Templer, R. H.; Seddon, J. M. *J. Phys.: Condens. Matter* **2006**, *18*, S1105. (c) Barauskas, J.; Johnsson, M.; Tiberg, F. *Nano Lett.* **2005**, *5*, 1615.
(12) Seddon, J. M.; Templer, R. H. Polymorphism of Lipid-Water Systems. In *Handbook of Biological Physics*; Lipowsky, R., Sackmann, E., Eds.; Elsevier Science, 1995; Vol. 1, Chapter 3, pp 97−160.
(13) Boyer, C. C.; Zasadzinski, J. A. *ACS Nano* **2007**, *1*, 176.
(14) (a) Yaghmur, A.; de Campo, L.; Sagalowicz, L.; Leser, M. E.; Glatter, O. *Langmuir* **2006**, *22*, 9919. (b) Rangelov, S.; Almgren, M. *J. Phys. Chem. B* **2005**, *109*, 3921.
(15) Yaghmur, A.; de Campo, L.; Salentinig, S.; Sagalowicz, L.; Leser, M. E.; Glatter, O. *Langmuir* **2006**, *22*, 517.
(16) de Campo, L.; Yaghmur, A.; Sagalowicz, L.; Leser, M. E.; Watzke, H.; Glatter, O. *Langmuir* **2004**, *20*, 5254.
(17) (a) Angelov, B.; Angelova, A.; Papahadjopoulos-Sternberg, B.; Lesieur, S.; Sadoc, J.-F.; Ollivon, M.; Couvreur, P. *J. Am. Chem. Soc.* **2006**, *128*, 5813. (b) Angelov, B.; Angelova, A.; Garamus, V. M.; Le Bas, G.; Lesieur, S.; Ollivon, M.; Funari, S.; Willumeit, R.; Couvreur, P. *J. Am. Chem. Soc.* **2007**, *129*, 13474.
(18) (a) Allen, T.; Cullis, P. R. *Science* **2004**, *303*, 1818. (b) Warriner, H.; Idziak, S.; Slack, N.; Davidson, P.; Safinya, C. *Science* **1996**, *271*, 969. (c) Warriner, H. E.; Keller, S. L.; Idziak, S. H. J.; Slack, N. L.; Davidson, P.; Zasadzinski, J. A.; Safinya, C. R. *Biophys. J.* **1998**, *75*, 272.
(19) (a) Lesieur, S.; Grabielle-Madelmont, C.; Menager, C.; Cabuil, V.; Dadhi, D.; Pierrot, P.; Edwards, K. *J. Am. Chem. Soc.* **2003**, *125*, 5266. (b) Martina, M.-S.; Fortin, J.-P.; Menager, C.; Clement, O.; Barratt, G.; Grabielle-Madelmont, C.; Gazeau, F.; Cabuil, V.; Lesieur, S. *J. Am. Chem. Soc.* **2005**, *127*, 10676.
(20) (a) Khodakov, A. Y.; Zholobenko, V. L.; Imperor-Clerc, M.; Durand, D. *J. Phys. Chem. B* **2005**, *109*, 22780. (b) Zeng, X.; Ungar, G.; Impéror-Clerc, M. *Nat. Mater.* **2005**, *4*, 562. (c) Kaneda, M.; Tsubakiyama, T.; Carlsson, Sakamoto, Y.; Ohsuna, T.; Terasaki, O. *J. Phys. Chem. B* **2002**, *106*, 1256. (d) Cherezov, V.; Clogston, J.; Papiz, M. Z.; Caffrey, M. *J. Mol. Biol.* **2006**, *357*, 1605.

10.1021/la804225j CCC: $40.75
Published on Web 02/17/2009

of nanoparticles, protein crystallization, hydrogels, functional foods, and nanostructured liquid crystalline (LC) systems.[2,6−8,20] In particular, the phase transitions involving cubic mesophase formation by surfactants and lipids exhibit considerable complexity.[21−33] They have attracted growing interest[34] and have provoked investigations focusing on their analogy with the mesophase transitions in di- and triblock copolymers forming LC structures.[35−39]

Even though liquid crystalline transitions to nonlamellar phases have been analyzed in a number of studies[8,10,12,31,33] and phase diagrams containing both isotropic and periodic phases in binary surfactant systems have been widely investigated by X-ray diffraction,[40−42] original time-resolved X-ray scattering curves demonstrating the dynamics of the transitions are insufficiently present in the literature.[21,22,32,43−50] Rich structural diagrams of lipid mesophases have been revealed with time-resolved X-ray diffraction scans employed to monitor the mesophase changes induced by pressure jumps.[47] The pressure jump experiments[47−50] have identified the existence of some unknown phases as intermediate structures during the lyotropic phase transformations that involve inverse bicontinuous cubic phases. In systems lacking full hydration, intermediate phases have been observed with concentrated surfactant solutions and at elevated temperatures.[51−54]

In the present work, the occurrence of an intermediate LC state during the thermal lamellar-to-double-diamond-cubic phase transition is reported at full hydration of the lipid in a lipid/surfactant/water dispersion. Time-resolved structural investigation is performed on self-assembly systems containing glycerol monooleate (MO), as the main amphiphile, and poly(ethylene glycol) monooleate (MO-PEG) or octyl glucoside (OG) surfactants serving as interfacial curvature modulators (Scheme 1). By means of synchrotron radiation small-angle X-ray scattering (SAXS), we study to what extent the fundamental structural features of the MO-PEG-functionalized assemblies may differ

Scheme 1. Molecular Models of the Investigated Nonionic Amphiphilic Molecules Glycerol Monooleate (MO), Poly(ethylene glycol) Monooleate (MO-PEG), and Octylglucoside (OG)

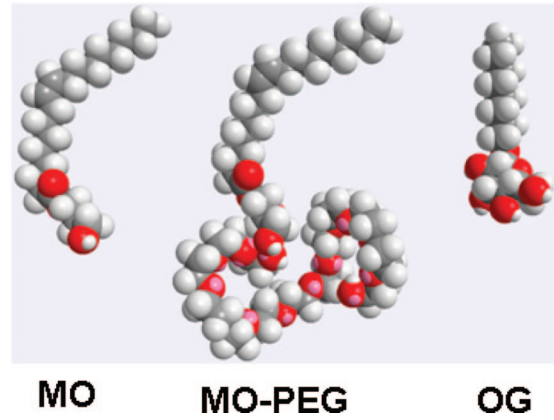

(21) Kraineva, J.; Narayanan, R. A.; Kondrashkina, E.; Thiyagarajan, P.; Winter, R. *Langmuir* **2005**, *21*, 3559.
(22) Persson, G.; Edlund, H.; Lindblom, G. *Eur. J. Biochem.* **2003**, *270*, 56.
(23) Imura, T.; Hikosaka, Y.; Worakitkanchanakul, W.; Sakai, H.; Abe, M.; Konishi, M.; Minamikawa, H.; Kitamoto, D. *Langmuir* **2007**, *23*, 1659.
(24) Dong, Y.-D.; Larson, I.; Hanley, T.; Boyd, B. J. *Langmuir* **2006**, *22*, 9512.
(25) (a) Popescu, G.; Barauskas, J.; Nylander, T.; Tiberg, F. *Langmuir* **2007**, *23*, 496. (b) Wörle, G.; Siekmann, B.; Koch, M. H. J.; Bunjes, H. *Eur. J. Pharm. Sci.* **2006**, *27*, 44. (c) Wörle, G.; Siekmann, B.; Koch, M. H. J.; Bunjes, H. *Eur. J. Pharm. Biopharm.* **2006**, *63*, 128.
(26) Spicer, P. T.; Hayden, K. L.; Lynch, M. L.; Ofori-Boateng, A.; Burns, J. L. *Langmuir* **2001**, *17*, 5748.
(27) Barauskas, J.; Misiunas, A.; Gunnarsson, T.; Tiberg, F.; Johnsson, M. *Langmuir* **2006**, *22*, 6328.
(28) Rosa, M.; Rosa Infante, M.; Miguel, M. d. G.; Lindman, B. *Langmuir* **2006**, *22*, 5588.
(29) Fong, C.; Wells, D.; Krodkiewska, I.; Weerawardeena, A.; Booth, J.; Hartley, P. G.; Drummond, C. J. *J. Phys. Chem. B* **2007**, *111*, 10713.
(30) (a) Pouzot, M.; Mezzenga, R.; Leser, M.; Sagalowicz, L.; Guillot, S.; Glatter, O. *Langmuir* **2007**, *23*, 9618. (b) Sakya, P.; Seddon, J. M.; Templer, R. H.; Mirkin, R. J.; Tiddy, G. J. T. *Langmuir* **1997**, *13*, 3706. (c) Mitchel, D. J.; Tiddy, G. J. T.; Waring, L.; Bostock, T.; McDonald, M. P. *J. Chem. Soc., Faraday Trans. 1* **1983**, *79*, 975.
(31) (a) Schwarz, U. S.; Gompper, G. *Phys. Rev. Lett.* **2000**, *85*, 1472. (b) Schwarz, U. S.; Gompper, G. *Langmuir* **2001**, *17*, 2084. (c) Schwarz, U. S.; Gompper, G. *J. Chem. Phys.* **2000**, *112*, 3792.
(32) Templer, R. H.; Seddon, J. M.; Duesing, P. M.; Winter, R.; Erbes, J. *J. Phys. Chem. B* **1998**, *102*, 7262.
(33) (a) Harper, P. E.; Gruner, S. M. *Eur. Phys. J. E.* **2000**, *2*, 217. (b) Garstecki, P.; Holyst, R. *Langmuir* **2002**, *18*, 2529–2537. (c) *ibid*, 2519−2528.
(34) (a) Leonard, M. J.; Strey, H. H. *Macromolecules* **2003**, *36*, 9549. (b) Olla, M.; Semmler, A.; Monduzzi, M.; Hyde, S. T. *J. Phys. Chem. B* **2004**, *108*, 12833. (c) Constantin, D.; Oswald, P.; Impéror-Clerk, M.; Davidson, P.; Sotta, P. *J. Phys. Chem. B* **2001**, *105*, 668. (d) Sallen, L.; Sotta, P.; Oswald, P. *J. Phys. Chem. B* **1997**, *101*, 4875.
(35) (a) Holmqvist, P.; Alexandridis, P.; Lindman, B. *Langmuir* **1997**, *13*, 2471. (b) Alexandridis, P.; Olsson, U.; Lindman, B. *Langmuir* **1997**, *13*, 23. (c) Alexandridis, P.; Olsson, U.; Lindman, B. *Langmuir* **1998**, *14*, 2627.
(36) Chatterjee, J.; Jain, S.; Bates, F. S. *Macromolecules* **2007**, *40*, 2882.
(37) (a) Imai, M.; Kawaguchi, A.; Saeki, A.; Nakaya, K.; Kato, T.; Ito, K.; Amemiya, Y. *Phys. Rev. E* **2000**, *62*, 6865. (b) Spontak, R. J.; Alexandridis, P. *Curr. Opin. Colloid Interface Sci.* **1999**, *4*, 140. (c) Bates, F. S. *Science* **1991**, *251*, 898.
(38) (a) Kunieda, H.; Kaneko, M.; Lopez-Quintela, M. A.; Tsukahara, M. *Langmuir* **2004**, *20*, 2164. (b) Zhu, L.; Huang, P.; Cheng, S. Z. D.; Ge, Q.; Quirk, R. P.; Thomas, E. L.; Lotz, B.; Wittmann, J.-C.; Hsiao, B. S.; Yeh, F.; Liu, L. *Phys. Rev. Lett.* **2001**, *86*, 6030. (c) Rodriguez-Abreu, C.; Shrestha, L. K.; Varade, D.; Aramaki, K.; Maestro, A.; Quintela, A. L.; Solans, C. *Langmuir* **2007**, *23*, 11007. (d) Bang, J.; Lodge, T. P. *Phys. Rev. Lett.* **2004**, *93*, 245701.
(39) (a) Hajduk, D. A.; Takenouchi, H.; Hillmyer, M. A.; Bates, F. S.; Vigild, M. E.; Almdal, K. *Macromolecules* **1997**, *30*, 3788. (b) Hajduk, D. A.; Gruner, S. M.; Rangarajan, P.; Register, R. A.; Fetters, L. J.; Honeker, C.; Albalak, R. J.; Thomas, E. L. *Macromolecules* **1994**, *27*, 490. (c) Hashimoto, T.; Nishikawa, Y.; Tsutsumi, K. *Macromolecules* **2007**, *40*, 1066. (d) Jinnai, H.; Sawa, K.; Nishi, T. *Macromolecules* **2006**, *39*, 5815.
(40) (a) Duesing, P. M.; Seddon, J. M.; Templer, R. H.; Mannock, D. A. *Langmuir* **1997**, *13*, 2655. (b) Templer, R. H.; Seddon, J. M.; Warrender, N. A.; Syrykh, A.; Huang, Z.; Winter, R.; Erbes, J. *J. Phys. Chem. B* **1998**, *102*, 7251. (c) Johnsson, M.; Barauskas, J.; Tiberg, F. *J. Am. Chem. Soc.;* **2005**, *127*, 1076. (d) Landh, T. *J. Phys. Chem.* **1994**, *98*, 8453.
(41) Oradd, G.; Gustafsson, J.; Almgren, M. *Langmuir* **2001**, *17*, 3227.
(42) Sato, T.; Hossain, Md. K.; Acharya, D. P.; Glatter, O.; Chiba, A.; Kunieda, H. *J. Phys. Chem. B* **2004**, *108*, 12927.
(43) (a) Czeslik, C.; Winter, R.; Rapp, G.; Bartels, K. *Biophys. J.* **1995**, *68*, 1423. (b) Funari, S. S.; Rapp, G. *Proc. Natl. Acad. Sci. U.S.A.* **1999**, *96*, 7756.
(44) Rappolt, M.; DiGregorio, G. M.; Almgren, M.; Amenitsch, H.; Pabst, G.; Laggner, P.; Mariani, P. *Europhys. Lett.* **2006**, *75*, 267.
(45) (a) Angelov, B.; Angelova, A.; Ollivon, M.; Bourgaux, C.; Campitelli, A. *J. Am. Chem. Soc.* **2003**, *125*, 7188. (b) Angelova, A.; Angelov, B.; Papahadjopoulos-Sternberg, B.; Ollivon, M.; Bourgaux, C. *Langmuir* **2005**, *21*, 4138. (c) Angelova, A.; Angelov, B.; Lesieur, S.; Mutafchieva, R.; Ollivon, M.; Bourgaux, C.; Willumeit, R.; Couvreur, P. *J. Drug Delivery Sci. Technol.* **2008**, *18*, 41–45.
(46) (a) Feng, Y.; Yu, Z.-Y.; Quinn, P. J. *Chem. Phys. Lipids* **2003**, *126*, 141. (b) Cherezov, V.; Siegel, D. P.; Shaw, W.; Burgess, S. W.; Caffrey, M. *J. Membr. Biol.* **2003**, *195*, 165.
(47) (a) Squires, A. M.; Templer, R. H.; Seddon, J. M.; Woenckhaus, J.; Winter, R.; Finet, S.; Theyencheri, N. *Langmuir* **2002**, *18*, 7384. (b) Squires, A.; Templer, R. H.; Ces, O.; Gabke, A.; Woenckhaus, J.; Seddon, J. M.; Winter, R. *Langmuir* **2000**, *16*, 3578.
(48) Conn, C. E.; Ces, O.; Mulet, X.; Finet, S.; Winter, R.; Seddon, J. M.; Templer, R. H. *Phys. Rev. Lett.* **2006**, *96*, 108102.
(49) Shearman, G. C.; Khoo, B. J.; Motherwell, M.-L.; Brakke, K. A.; Ces, O.; Conn, C. E.; Seddon, J. M.; Templer, R. H. *Langmuir* **2007**, *23*, 7276.
(50) Paccamiccio, L.; Pisani, M.; Spinozzi, F.; Ferrero, C.; Finet, S.; Mariani, P. *J. Phys. Chem. B* **2006**, *110*, 12410.
(51) Holmes, M. C.; Leaver, M. S. Intermediate Phases. In *Bicontinuous Liquid Crystals* (Surfactant Science Series),; Lynch, M. L., Spicer, P. T., Eds.; Taylor & Francis: Boca Raton, 2005; Vol. 127, pp 15−39.
(52) (a) Baciu, M.; Holmes, M. C.; Leaver, M. S. *J. Phys. Chem. B* **2007**, *111*, 909. (b) Wang, Y.; Holmes, M. C.; Leaver, M. S.; Fogden, A. *Langmuir* **2006**, *22*, 10951.
(53) (a) Funari, S. S.; Holmes, M. C.; Tiddy, G. J. *J. Phys. Chem.* **1994**, *98*, 3015. (b) Funari, S. S.; Holmes, M. C.; Tiddy, G. J. *J. Phys. Chem.* **1992**, *96*, 11029. (c) Fairhurst, C. E.; Holmes, M. C.; Leaver, M. S. *Langmuir* **1997**, *13*, 4964. (d) Holmes, M. C.; Leaver, M. S.; Smith, A. M. *Langmuir* **1995**, *11*, 356.
(54) Hamley, I. W.; Castelletto, V.; Mykhaylyk, O. O.; Yang, Z.; May, R. P.; Lyakhova, K. S.; Sevink, G. J. A.; Zvelindovsky, A. V. *Langmuir* **2004**, *20*, 10785.

from those of the pure lipid component (MO) hydrated in excess aqueous environment. The lamellar-to-double-diamond-cubic phase transition mechanism in the presence of the MO-PEG derivative, which could induce membrane curvature perturbations and defects in the lipid bilayer, is studied. In view of the perspective to prepare sterically stabilized nanoparticles with internal structure, we wanted to establish whether the addition of a MO-PEG derivative predominantly influences the order-order lamellar-to-cubic and cubic-to-hexagonal transitions of MO or provokes bilayer curvature changes and distortions which might favor other phases. In the two-component MO/MO-PEG and MO/OG amphiphilic systems, long-living intermediate states were identified as a weakly ordered cubic phase coexisting with a sponge-like bicontinuous phase. The temperature-induced intermediate states in the MO/MO-PEG mixture were compared with the long-living intermediates obtained via thermal cycling and storage conditioning of a MO/OG sample forming a swollen double-diamond cubic phase under full hydration.[17b,45a]

Materials and Methods

Poly(ethylene glycol) monooleate (MO-PEG) (average $M_n \sim 860$, density 1.034 g/mL at 25 °C) was purchased from Aldrich, octylglucoside (OG) from Fluka Biochemica (>99%), and powder of oleoyl-*rac*-glycerol (MO) from Sigma (purity 99%). The inorganic salts (NaH_2P0_4, Na_2HPO_4, NaCl), all of p.a. grade, were received from Fluka. The organic solvent chloroform (Merck) was of p.a. grade as well. The chemicals were used as received.

Amphiphilic dispersion samples were prepared via self-assembly in excess buffer phase (30 wt. % solid, 70 wt. % buffer) under conditions that avoid high-energy input. The experimental protocol for the MO/MO-PEG system included weighting and mixing of the amphiphilic components at a molar ratio 90/10 in chloroform, evaporation of the solvent under nitrogen gas flow, and subsequent overnight lyophilization aiming at elimination of eventually remaining traces of chloroform. The self-assembly was achieved by employing repeated cycles of vortexing and equilibration after hydration of the dried MO/MO-PEG mixture in phosphate buffer salt solution (0.1 M NaCl, phosphate pH 7).

Spontaneously self-assembled MO/OG (90/10 and 85/15 mol/mol) systems were prepared according to a previously reported experimental procedure.[17b] The MO/OG 90/10 system forms initially a D_{Large} swollen diamond cubic phase at low and room temperatures. After heating to 55 °C, the transition $D_{Large}-D_{Normal}$ occurs as described earlier.[17b,45a] The sample investigated here was subjected to a thermal cycling sequence: cooling to 1 °C−heating to 55 °C−cooling to 23 °C. Then a SAXS pattern was measured at room temperature (23 °C). The recovery of the D_{Large} phase from a D_{Normal} cubic phase appears to be a slow process and permitted us to investigate the intermediate states in the cooling step to room temperature. Particular equilibration and thermal conditioning was done also with the sample MO/OG 85/15 (mol/mol). After 8 months of storage at 1 °C, its structural organization was investigated in a heating scan from 1 to 68 °C.

For small-angle X-ray scattering (SAXS) experiments, the samples were filled in glass mark tubes with diameters of 1 or 4 mm. Beamlines B1 and A2 at HASYLAB (DESY, Hamburg) and D24 at LURE (Orsay) were used. In time-resolved SAXS measurements, individual frames were recorded at a scan rate of 2 °C/min in the temperature interval from 1 to 68 °C. The scattering intensities were corrected for background. The calibration of the q-scale in the SAXS patterns was done using tristearin ($d_{001} = 4.497$ nm) and silver behenate ($d_{001} = 5.838$ nm). The length of the scattering vector, q, is defined as

$$q\ (\text{Å}^{-1}) = (4\pi/\lambda)\ \sin(\theta) = 2\pi/d$$

where 2θ is the scattering angle; $\theta = 1.5$ Å is the X-ray wavelength; and d is the repeat spacing.

The radius of gyration of the PEG chains was calculated using the CRYSOL software.[55] This program calculates spherically averaged X-ray scattering patterns of macromolecules in water solution. It reads the atomic coordinates of the macromolecule presented in a Protein Data Bank format. In addition to the scattering pattern, the program can calculate structural parameters such as the radius of gyration, volume, and molecular weight of the macromolecule.

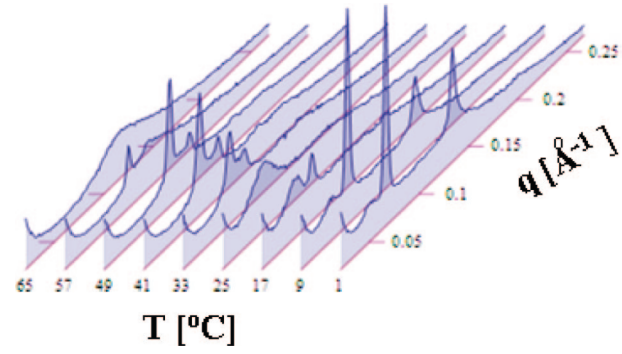

Figure 1. Selected frames from the Synchrotron radiation small-angle X-ray scattering vs temperature scan recorded at a scan rate of 2 °C/min upon heating of a MO/MO-PEG (90/10 mol/mol) spontaneously self-assembled mixture in the interval from 1 to 68 °C. The system exhibits well-defined intermediate states during the transition from a lamellar to a diamond cubic phase (space group Pn3m).

Results

1. Phase Behavior of a Spontaneously Self-Assembled MO/MO-PEG Mixture Revealing Long-Living Intermediates as a Cubic Phase Precursor at Full Hydration. The thermotropic structural behavior of the MO/MO-PEG (90/10, mol/mol) dispersion in excess buffer environment was investigated by a SAXS temperature scan between 1 and 68 °C. Figure 1 presents selected patterns, which indicate that the transition from a lamellar to a bicontinuous cubic phase in the studied two-component system is not instantaneous. It differs from the narrow (1 °C) transformation found in other binary lipid mixtures.[56] In fact, it does not come up like a sharp jump or a discontinuous switch between lamellar and cubic phases. This thermally induced transition appears to be a rather slow and smooth transformation in which long-living intermediate structures coexist within broad temperature (several degrees Celsius: from 1 to 31 °C) and time intervals (several minutes: for instance 15 min at a scan rate of 2 °C/min).

While the pure lipid MO forms at low temperatures (T < 15 °C) a single lamellar phase[6b] upon hydration in 0.1 M NaCl salt buffer environment, the inclusion of the MO-PEG additive in the self-assembly system induces a coexistence of the lamellar structure with a peak of a second phase positioned at a small q-distance. This swollen structure is considered to be a long-living intermediate state being a cubic phase precursor. The dynamic scan in Figure 1 indicates that the structural intermediates are present in the L−D transition as a long-living metastable phase rather than as millisecond transient states.

The position of the lamellar Bragg peak (Figure 1, frame 1) corresponds to a repeat spacing $d_{001} = 9.37$ nm at 1 °C (Table 1), which decreases to $d_{001} = 8.84$ nm upon heating to 15 °C. These lamellar spacings are essentially bigger in comparison to the value for pure MO, $d_{001} = 5.04$ nm, which is almost temperature invariant.[6b] Raising the temperature above 19 °C leads to complete transformation of the lamellar domain into a long-living intermediate state characterized by broad scattering

(55) Svergun, D. I.; Barberato, C.; Koch, M. H. J. *J. Appl. Crystallogr.* **1995**, *28*, 768.
(56) Ishoy, T.; Mortensen, K. *Langmuir* **2005**, *21*, 1766.
(57) Teubner, M.; Strey, R. *J. Chem. Phys.* **1987**, *87*, 3195.

Table 1. Temperature Dependence of the Characteristic SAXS Distances for a Lamellar (L) Phase, an Intermediate Long-Living Phase, a Double-Diamond Cubic Phase (Pn3m Space Group), and an Isotropic Fluid State Thermally Induced in Fully Hydrated MO/MO-PEG (90/10, mol/mol) Self-Assemblies[a]

T (°C)	1st peak of the intermediate phase q (Å^{-1})	lamellar phase q_{001} (Å^{-1})/d_{001} [nm]	cubic Pn3m phase q_{110} (Å^{-1})/a [nm]	isotropic fluid q (Å^{-1})/d_M [nm]
1	0.049	0.067/9.37		
5	0.051	0.067/9.37		
10	0.051	0.068/9.23		
15	0.053	0.071/8.84		
20	0.057			
25	0.063			
30	0.066			
35			0.071/12.52	
40			0.078/11.39	
45			0.083/10.70	
50			0.088/10.09	
55			0.087/10.21	
60				0.112/5.61
65				0.119/5.28

[a] The SAXS peak position is defined by the scattering vector q. The lattice spacings are denoted as d_{001} (for the lamellar phase) and a (for the cubic phase). The characteristic distance of the isotropic liquid phase is denoted as d_M.

peaks. In the temperature range from 19 to 31 °C, there is a lack of sharp Bragg reflections characteristic of single-crystal liquid-crystalline domains.

Table 1 summarizes the peak position maxima of the intermediate phase located in the range from $q = 0.049$ to $q = 0.066$ Å^{-1}. These q-values, below 0.07 Å^{-1}, confirm that the intermediate is a very swollen state and that the steric repulsion caused by the MO-PEG additive results in water compartment enlargement. The SAXS patterns of the intermediate states recorded at $T = 23$ °C and at $T = 31$ °C are presented in Figure 2a (curves 1 and 2). They are considered in more detail in the following section where the long-living intermediates are compared with other binary amphiphilic systems containing glycerol monooleate as the main component (Figure 2b). It should be recalled that in lipid/surfactant systems missing cubic phase formation the swollen intermediate state (characterized by broad diffusive scattering at low q-values) has been associated with scattering from water-filled defects in the lamellas and the formation of a random mesh lamellar (L_α^h) phase with 2D topology.[41,52a]

The growth of bicontinuous cubic domains from the intermediate state in the MO/MO-PEG system is established upon heating to temperatures above $T = 33$ °C (Figure 1). Bragg diffraction peaks confirm the long-range liquid-crystalline order. The indexing of the observed diffraction peaks reveals that the growing phase is a double diamond bicontinuous cubic phase (space group Pn3m) (see Figure 1S in Supporting Information). The characteristic spacing determined at temperature 40 °C ($a = 11.39$ nm) (Table 1) is bigger than that of the D_{Normal} (Pn3m) cubic phase of the pure MO/water assembly ($a = 9.19$ nm at 40 °C).[6b] This increase appears to be caused by the inclusion of the MO-PEG component in the lipid bilayer.

The SAXS data indicate that 10 mol % of MO-PEG in the amphiphilic mixture is sufficient to modify the structural features of the spontaneously formed binary LC assembly with regard to the pure glycerol monooleate/water system.[6b,43a] Diffraction peaks from an inverted hexagonal (H_{II}) phase were not detected in the investigated temperature range. At $T > 57$ °C, the cubic phase begins to melt to an isotropic liquid state (probably an L_2 phase).

Macroscopic phase segregation between the two amphiphilic components was not established in the investigated nanostructured system. The distribution of the MO-PEG constituent, possessing a bulky hydrophilic group, appears to be random (without macroscopic domains) along the MO/MO-PEG bilayer membrane.

The phase sequence derived from the performed time-resolved temperature scan (Figure 1), in which the observed transitions occur in broad temperature ranges, is

$$\text{lamellar (L)} + \text{swollen intermediate} \xrightarrow{19\ ^\circ\text{C}} \text{long-living intermediate} \xrightarrow{33\ ^\circ\text{C}} \text{cubic Q}^{224}\ \text{(Pn3m)} \xrightarrow{61^\circ\text{C}} \text{isotropic fluid}$$

With the two-component MO/MO-PEG amphiphilic mixture, the lamellar-to-cubic transition goes through a swollen intermediate phase (Figures 1 and 2a). The latter is suggested to represent the onset of the large-scale ordering that precedes the temperature-induced transition of the dense lipid nanodispersion into cubic lattice domains. The nucleation and growth of cubic-lattice LC structures appear to occur with longer induction times in such binary amphiphilic codispersions.

2. Similarity of the SAXS Patterns of Long-Living Intermediates in MO/MO-PEG Self-Assemblies with Those in Thermally Cycled or Long-Term Equilibrated MO/OG Mixtures. To find out whether the intermediate phase is specific to the MO-PEG amphiphile, we investigated self-assemblies in which the surfactant OG replaced the MO-PEG derivative (see Materials and Methods for the equilibration and thermal history of the MO/OG samples). This section focuses on the SAXS pattern shapes and peak positions in the scattering curves of the MO/OG (85/15, mol/mol) assembly equilibrated for 8 months at 1 °C (Figure 2b). In the temperature range 42−54 °C, the aged system forms a stable swollen intermediate, which does not crystallize into a cubic lattice upon further heating and dehydration at high temperatures.

Figure 2 shows SAXS curves of long-living intermediates formed in hydrated MO/MO-PEG (90/10, mol/mol) (Figure 2a) and MO/OG (85/15, mol/mol) (Figure 2b) binary self-assembly mixtures. The two systems differ in their chemical and molar compositions as well as in their thermal history, aging conditioning, and geometric shape of the nonionic surfactant additives. However, the SAXS patterns in Figure 2a (curves 1−2) and Figure 2b (curves 4−5) display remarkable similarity of their forms as well as of their thermal behavior.

Every SAXS pattern of an intermediate state presented in Figure 2 is constituted by two broad and distinct scattering peaks. The first one, centered at a low q-value around 0.06 Å^{-1}, is narrower in width, and it is stronger in intensity. The second broad scattering peak is weaker, and it is centered at a q-value around 0.13 Å^{-1}. The first peak is temperature sensitive. It shifts from 0.05 to 0.07 Å^{-1} upon raising the temperature up to 31 °C (Figure 2a) or up to 54 °C (Figure 2b). This shift to larger q-values (respectively, to smaller distances) is known in the literature on liquid crystalline phases.[2b]

The dehydration of the MO/MO-PEG assembly upon heating is associated with a transition of the swollen intermediate phase (the cubic-phase precursor) into a bicontinuous cubic liquid-crystalline structure at $T > 33$ °C (Figure 2a, pattern 3). Owing to the fact that the second broad peak ($q \sim 0.13$ Å^{-1}) does not display a well-defined maximum, its temperature sensitivity could not be precisely followed. This bump in the SAXS patterns seems to be unaffected by temperature changes.

The comparison of the patterns of the intermediate phases in MO/MO-PEG (Figure 2a, patterns 1 and 2) and in MO/OG self-assemblies (Figure 2b, patterns 4 and 5) indicates that the nature of the surfactant additive does not have a specific influence on

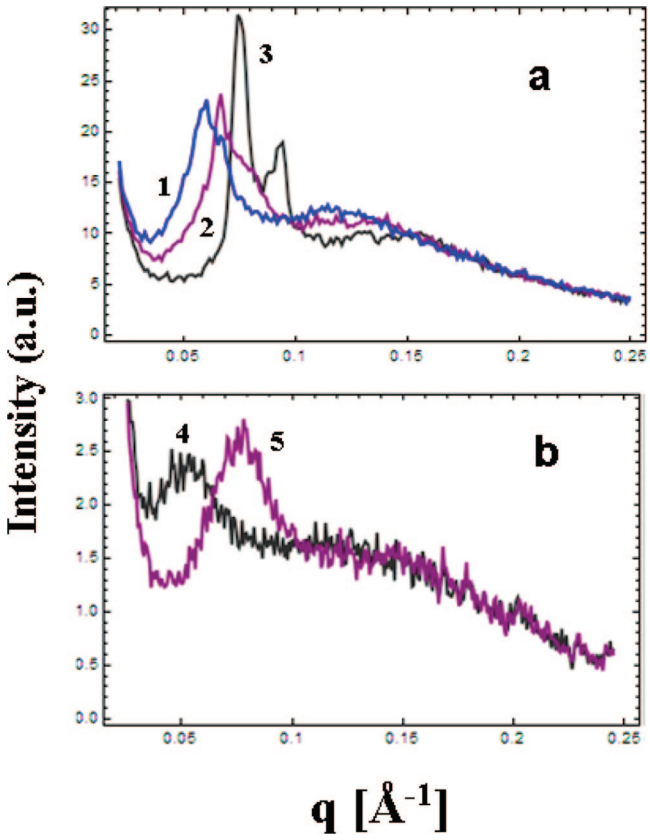

Figure 2. (a) Small-angle X-ray scattering curves characteristic of the intermediate states that are thermally induced in a MO/MO-PEG (90/10 mol/mol) assembly. The peak maxima are at $q = 0.059$ Å^{-1} for $T = 23$ °C (pattern 1, blue curve) and $q = 0.066$ Å^{-1} at $T = 31$ °C (pattern 2, purple curve). Pattern 3 is recorded at $T = 39$ °C (black curve) and corresponds to a diamond cubic phase (Pn3m space group) with a cubic lattice parameter $a = 11.84$ nm. (b) Selected SAXS patterns from the thermal scan of the MO/OG (85/15 mol/mol) self-assembly mixture equilibrated for 8 months at 1 °C and scanned upon heating. The peak maxima of the intermediate are at $q = 0.054$ Å^{-1} for $T = 42$ °C (pattern 4, black curve) and $q = 0.077$ Å^{-1} for $T = 54$ °C (pattern 5, purple curve).

the shape of the scattering curves nor on the position of the second broad scattering bump centered at q around 0.13 Å^{-1}. As the MO-PEG and OG components have a role of hydration- and interfacial-curvature modulators, they display a primary influence on the diffusive scattering at low q-values. The intensity maximum is at q around 0.055 Å^{-1} (pattern 4 in Figure 2b) at temperature 42 °C. It is located at the almost same q-value as with the MO-PEG additive (pattern 1 in Figure 2a). After raising the temperature to 54 °C (pattern 5 in Figure 2b), the first peak position shifts to the higher q-range. This behavior is analogous to that of the MO/MO-PEG mixture (pattern 2 in Figure 2a).

Taking into account the markedly different geometry of the two surfactant additives (OG and MO-PEG), a conclusion can be drawn that the intermediate state is not a particular MO/OG or MO/MO-PEG feature. It is a characteristic kind of a highly hydrated and weakly structured state that corresponds to a three-dimensional bilayer network being a cubic phase precursor. Due to its high molecular weight, the MO-PEG amphiphile is capable of extending the life of the intermediate state. In the case of OG, the thermal cycling and the long equilibrium period of the sample (8 months) facilitate the stabilization of the intermediate phase over extended time and thus completely destabilize the cubic LC phase after the 8 month aging period.

At maximum swelling in an excess aqueous medium, the glycerol monooleate LC assembly attains a scattering intensity maximum at a q-value as small as 0.05 Å^{-1} (Figure 2). It should be recalled that the maximum swelling of the diamond D_{Large} cubic lattice, induced by the hydration enhancer OG in the MO/OG 90/10 cubic membrane, was found to yield[45a] $a = 15.3$ nm. The above-indicated features suggest that the long-living intermediate appears to be a general characteristic of the lamellar-to-cubic structural phase transition in binary amphiphilic mixtures. The MO-PEG amphiphile tends to slow the kinetics of the transition to a cubic phase via its influence on the hydration and on the packing ordering.

3. Background Scattering Analysis of Long-Living Intermediates Involving Weakly Ordered Cubic and Sponge-Like Phases. Figure 2 demonstrates that an essential feature of the long-living intermediates is the large diffusive scattering background in their SAXS patterns. For MO assemblies, such enhanced scattering background has been previously attributed[33] to formation of a microemulsion-like phase (see section 3.1 in ref 33b, p 2531). In fact, the "emulsion-like" scattering background[33b] is frequently present in SAXS experiments conducted with MO-rich systems at $T < 25$ °C. In the case of a lamellar-to-cubic phase transformation, this scattering background should be subtracted from the pattern of the cubic phase to evaluate the diffraction intensity resulting from the periodic self-assembly nanostructure (an absolute SAXS intensity, presented in [cm^{-1}] units, is needed for the correct subtraction of the background resulting from the aqueous buffer phase and the capillary).

Figure 3a shows a SAXS pattern recorded at room temperature ($T = 23$ °C) with a long-living intermediate generated with a fully hydrated MO/OG (90/10, mol/mol) assembly following a thermal cycling (for sample preparation, see Materials and Methods). This molar composition was chosen for SAXS pattern analysis because it avoids the lamellar peak that is present in the patterns of the MO/OG 85/15 assembly at low temperatures[17b] masking the scattering that could arise from an eventually formed "emulsion-like"[33b] phase.

Here we measured the absolute SAXS intensities during the slow phase transition of an intermediate into a D_{Normal} cubic phase. The diffusive scattering background in the presently investigated binary system appears to be related to the growth of a swollen cubic phase. In the SAXS pattern in Figure 3a, one observes the resulting characteristic scattering peaks of the intermediate. The two broad bumps centered at $q = 0.063$ Å^{-1} and at $q = 0.13$ Å^{-1} essentially differ from narrow Bragg diffraction reflections. The second peak at a q-value around 0.13 Å^{-1} resembles in shape a scattering curve from liquid-crystalline organization with low order.

To fit the SAXS patterns of the swollen intermediate (Figure 3a), we plotted the intensity, $I(q)$, as a sum of the scattering from a double-diamond cubic phase and from bilayer sponge cell−cell correlations. The total scattering was calculated according to the equation

$$I(q) = \frac{c_1}{q^2}\sum_{hkl} \exp\left[-\frac{(q - q_{hkl})^2}{2\sigma^2}\right] I_{hkl} + \frac{c_2}{\xi^{-2} + (q - q_c)^2} \quad (1)$$

where the first term describes the cubic phase scattering (see the scattering model in ref 33b) and the second term corresponds to the bilayer cell−cell correlations (see eq 2 in ref 3b). The peak positions are denoted by q_{hkl} and q_c. The peak widths for all peaks of the cubic phase are considered to be the same and described by σ. The correlation length is ξ, while the constants c_1 and c_2 describe the intensity normalization. The cubic phase individual peak maximal intensities are given by I_{hkl}.

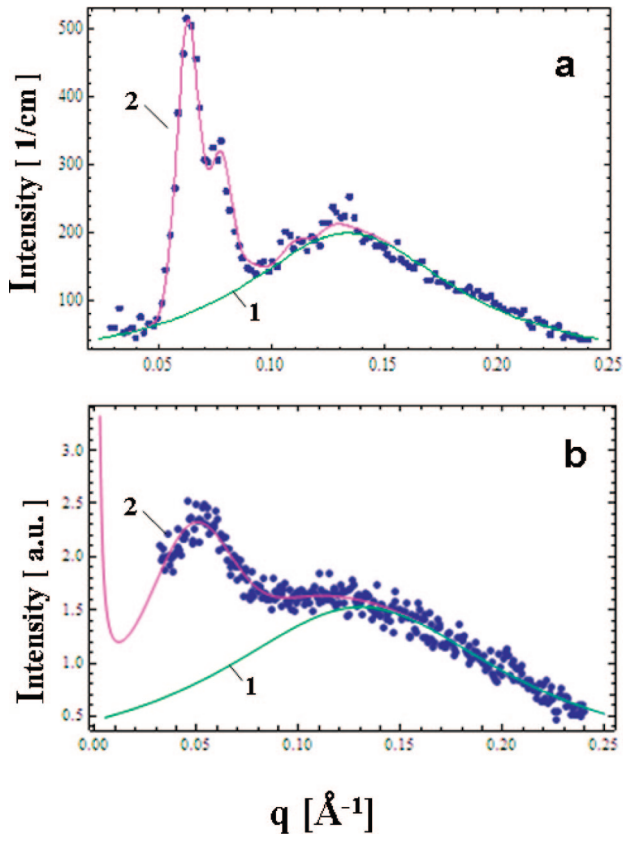

Figure 3. (a) Absolute X-ray scattering intensity from an intermediate state generated with a MO/OG (90/10 mol/mol) self-assembly nanodispersion. The maximal intensity is at $q = 0.063$ Å^{-1} at $T = 23$ °C, and it should correspond to a swollen cubic precursor with a Pn3m lattice ($a = 14.1$ nm). (b) Normalized SAXS pattern for the system MO/OG (85/15 mol/mol, curve 4 from Figure 2b). For both systems, the upper pattern 2 (purple color) is a fit according to eq 1. The lower pattern 1 (green color) represents the model scattering of the bilayer sponge cell−cell correlations (see the right term in eq 1).

A detailed comparison between the scattering calculated using a microemulsion model, a bilayer sponge cell−cell correlation, and a Gaussian function is given in the Supporting Information (Figures 4S, 5S, and 6S). It permitted us to select the sponge-like scattering[3b] as the best-fit model (instead of the microemulsion background).[33b] In Figure 3, the presented sponge scattering pattern (curve 1) was obtained with a value $q_c = 0.133$ A^{-1}. The scattering from the cubic phase (curve 2) was fitted with a Pn3m cubic symmetry. Its parameters, a bilayer thickness of 3.2 nm and a unit cell size of 14.1 nm, correspond to a water channel diameter of 6.77 nm and a peak width parameter of $\sigma = 0.0049$. The fact that the broad scattering bump at large q-values ($q \sim 0.13$ Å^{-1}) could be fitted with a bilayer sponge cell−cell correlation, as a background, does not necessarily imply that it is an integral part of the intermediate in the MO assemblies. It may suggest the presence of domains during the phase transition as the scattering from the intermediate states can be decomposed into cubic plus sponge-like scattering.

Figure 3b presents the best fit of the SAXS curve 4 from Figure 2b according to the model employed here. The position of the cell−cell correlation peak was found to be almost the same, i.e., $q_c = 0.131$ A^{-1} (curve 1). The cubic phase term (curve 2, Pn3m space group) was fitted with a bilayer thickness of 3.3 nm, unit cell size of 15.6 nm, and a peak width parameter $\sigma = 0.0167$. In this case, σ is more than 3 times bigger than the peak width parameter in the previous system ($\sigma = 0.0049$, Figure 3a) indicating very weak ordering of the cubic phase in Fugure 3b.

In the Supporting Information, we present simulated cubic phase diffraction patterns obtained at different values of the peak width parameter σ (Figure 3S).

Discussion

Soft matter nanomaterials, which are often functionalized supramolecular amphiphilic assemblies or codispersions of two or more lipids and/or surfactants in an appropriate solvent, are commonly characterized by nanoscale−nonuniform distribution of the components. Such binary or polycomponent systems have been indicated to form intermediate phases in their structural phase diagrams.[40b,47,53] Intermediate transient phases have generally been reported under nonequilibrium conditions associated with phase transformations at limited hydration.[51−53] It should be taken into account that lattice deformations, bilayer distortions or disruptions, and membrane curvature inhomogeneity are common for two- and multicomponent self-assembly lipid structures.[17a,18b,c,37a,53c]

With pure nonlamellar lipid/water systems, the general phase sequence may involve sharp transitions between diverse structural organizations[12]

Lamellar (L) − Cubic (Q) − Inverted Hexagonal (H_{II}) − Isotropic (I)

In time-resolved SAXS measurements, transition intermediates in concentrated aqueous monoglyceride dispersions have been observed at relatively short time scales under nonequilibrium conditions.[21] Dynamic temperature scans in pressure jump experiments have induced a phase conversion into nonequilibrium supramolecular lipid structures.[47,50] However, such intermediate states have not been conserved as equilibrium phases upon sample storage. SAXS studies have indicated that transient intermediate states are more apparent with binary lipid/surfactant mixtures[40b,47] at variance to the phase transition sequences of single-lipid dispersions.[21,40a,56] In the latter case, the phase behavior is rather rich, but it is often represented by structural arrangements in a two-state order−order transition[21] instead of weakly structured intermediates. The phase transition kinetics in pure monoglyceride/water systems is expected to be considerably faster in the manner that single-crystal domains of the new nonlamellar phase would nucleate and grow more effortlessly with regard to those in binary monoglyceride/surfactant mixtures. The growth of single-crystal domains is largely hampered in binary or multicomponent liquid crystalline systems, where the perturbations of the lipid bilayer membranes and the enhanced hydration play a role.[17b]

Molecular Packing Considerations for the MO/MO-PEG Mixture. Theoretical approaches[9,51] have related the occurrence of intermediate phases to the molecular shapes that govern the hydrophobic/hydrophilic balance of the amphiphiles, the geometrical mismatches, and the packing constrains in their mixtures. For instance, intermediate phases have been predicted to replace the bicontinuous cubic phases in mixtures of nonionic surfactants involving polyoxyethylene headgroups[52b] and relatively short alkyl chain homologues (e.g., $C_{16}EO_6$). Unbalanced competition between hydrophobic chain length and surface packing has been suggested to cause the formation of intermediate LC structures with various morphologies.[52b]

The established absence of phase separation between the MO and MO-PEG amphiphiles (Figure 1) allowed estimating the critical packing parameter, $<\eta>$, of the investigated binary system at a molar ratio 90/10. For individual chemical species, η_i is defined as

Table 2. Molecular Packing Parameters, η_i, of the MO and MO-PEG Amphiphiles Estimated from the Hydrophobic Oleyl Chain Volume (v_H), the Hydrophobic Chain Length, l, and the Cross-Sectional Headgroup Area, A

	MO	MO-PEG
l_H (nm)	1.86	1.86
v_H (nm^3)	0.476	0.476
A (nm^2)	0.24	1.58
η_i	1.07	0.16

$$\eta_i = v_H/Al \quad (2)$$

where v_H is the volume of the hydrophobic oleyl chains with chain length l, and A is the cross-sectional headgroup area involving the PEG chain or the polar glycerol group of MO, respectively. Considering MO-PEG as a pseudosingle component with a hydrophilic chain of oxyethylene (EO) units, one gets the structural data presented in Table 2. The area per hydrophilic moiety was estimated using the gyration radius of the PEG chain ($R_g = 7.1$ Å) calculated by means of the CRYSOL software.[55]

Based on the assumption for molecular miscibility, the critical packing parameter, $<\eta>$, of the MO/MO-PEG (90/10, mol/mol) mixture was calculated as the weighted average value:

$$<\eta> = X_1\eta_1 + X_2\eta_2 \quad (3)$$

where X_1 and X_2 are the mole fractions of the amphiphiles in the binary mixture. The obtained packing parameter, $<\eta>$, is slightly smaller than unity ($<\eta> = 0.979$) and explains the presence of a lamellar phase in the system at low temperatures. The critical concentration, defining the stability of the lamellar phase before its transition to a curved nonlamellar phase, was determined to be 7.5 mol % MO-PEG, the MO-PEG additive being the interfacial curvature modulator.

In the presently studied MO/MO-PEG system, the applied thermal stimulus likely induces, at a molar ratio 90/10, a random nonuniformity of the interfacial monolayer curvature without macroscopic phase separation between the two components. Both the conformation and the hydration of the EO chains are temperature sensitive.[58] This kind of hydrophilic moiety dehydrates with increasing temperature, which influences the overall phase behavior of the binary mixtures. As the hydration and the conformation of the headgroups (influencing the molecular architecture) are temperature sensitive,[58] the dehydration of the EO chains could decrease the surface curvature. Therefore, in the binary mixture, the intermolecular interactions and packing were temperature modulated to achieve a preferred interfacial curvature permitting stabilization of a weakly ordered intermediate phase.

Topological Mechanism of the Lamellar-to-Cubic Phase Transition Involving Nonepitaxially Formed Long-Living Intermediates. The investigated self-assembly MO/MO-PEG (90/10) mixture forms long-living structural intermediates in a wide temperature range from 19 to 33 °C (Figure 1). At low temperatures, the intermediate phase coexists with a lamellar phase, while at high temperatures, it transforms to a cubic phase. The kinetics of nucleation and growth of an ordered bicontinuous cubic phase appeared to be considerably slowed down owing to the presence of the MO-PEG additive.

Table 1 indicates that the guest MO-PEG component induces, at low temperatures, a notable increase of the lamellar spacing of the binary amphiphilic assembly as compared to the repeat spacing of the pure MO lamellae[6b] ($d = 5.04$ nm, $q = 0.124$ Å^{-1}). Owing to the mismatch between the spacings of the MO/MO-PEG lamellae ($q = 0.071$ Å^{-1}) and the growing nonlamellar phase ($q = 0.053$ Å^{-1}) at $T > 15$ °C, the transition to an ordered diamond-type cubic phase with a dense {110} cubic plane with $q = 0.071$ Å^{-1} was hampered (Figure 1). To overcome the huge lattice mismatch during the lamellar-to-cubic (L−D) transition, an intermediate linking state was established. Thus, we could not experimentally observe an epitaxial relationship between the {110} plane of the diamond (D) cubic lattice and the lamellar {001} plane (Figure 4). The {110} plane of the D phase did not directly form from the lamellar plane. With the investigated binary amphiphilic mixture, an L−D epitaxiallity was not possible for the {211} plane of the D cubic lattice. In this system, the position of the (211) reflection of the D phase does not coincide with that of the L phase. The obtained results indicate that intermediate metastable states seems to be favored when epitaxial relationships are not straightforward and when the phase transformations are associated with energy barriers. The mismatch between the L and D lattice spacings is geometrically adjusted through an intermediate phase that is present over very broad temperature and time intervals.

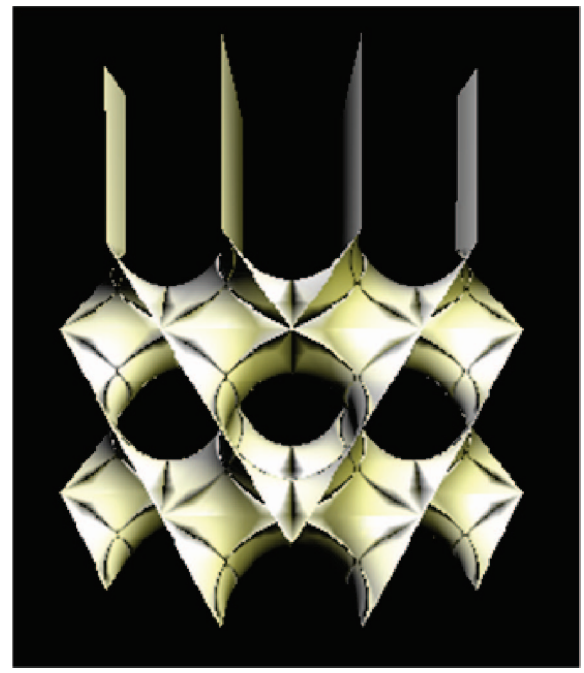

Figure 4. Geometrical presentation of an epitaxial relationship between lamellar and double diamond cubic lattices during a lamellar-to-diamond-cubic phase transition in a liquid crystalline system.

In contrast, epitaxiality has been established with single surfactant/water lyotropic LC phases.[59,60] For instance, epitaxial growth of a lamellar (L) from a gyroid (G) cubic phase and of a hexagonal (H) from a G phase has been reported for the surfactant $C_{12}EO_6$/water system.[60a,53a] The G{211} plane is epitaxially related with the L{001} plane and with the {10} plane of the H phase. In such pure surfactant systems, the G{111} plane yields hexagonally packed-cylinder growth upon application of external stimulus.

The organization of the swollen nonlamellar state, corresponding to the experimental scattering curves in Figures 2 and 3, could not be presented as a well-defined periodic structure due

(58) (a) Shigeta, K.; Olsson, U.; Kunieda, H. *Langmuir* **2001**, *17*, 4717. (b) Kunieda, H.; Shigeta, K.; Ozawa, K. *J. Phys. Chem. B* **1997**, *101*, 7952.

(59) (a) Luzzati, V. *J. Phys. II France* **1995**, *5*, 1649. (b) Fogden, A.; Hyde, S. T. *Eur. Phys. J. B* **1999**, *7*, 91. (c) Pieranski, P.; Sittler, L.; Sotta, P.; Imperor-Clerc, M. *Eur. Phys. J. E* **2001**, *5*, 317.

(60) (a) Rançon, Y.; Charvolin, J. *J. Phys. Chem.* **1988**, *92*, 2646–2651. (b) *ibid*. 6339−6344. (c) Clerc, M.; Levelut, A. M.; Sadoc, J. F. *J.Phys. II (France)* **1991**, *1*, 1263.

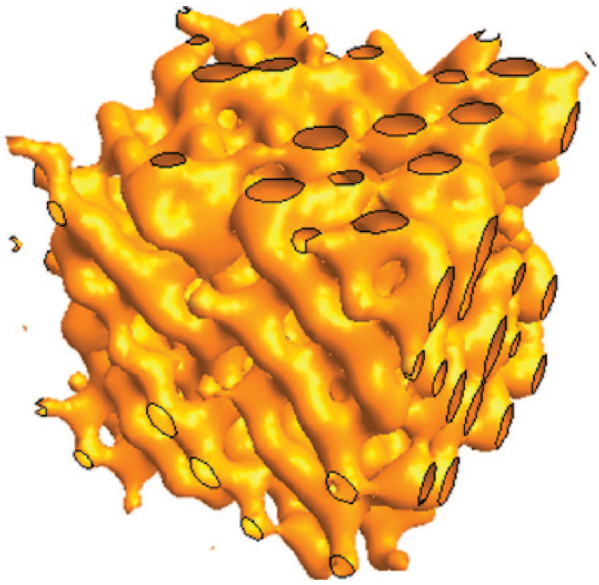

Figure 5. Nodal surface representation of the intermediate between a lamellar and a bicontinuous cubic phase of a space group Pn3m.

to the absence of strong Bragg diffraction peaks. The SAXS patterns are dominated by strong diffusive scattering. Previously, the small-angle diffusive scattering from nonionic surfactant self-assemblies or block copolymer lamellas has been explained as due to water-filled pores in the lamellas (e.g., perforated bilayers in mesh phases).[52,54] While the results obtained in the present work suggest the existence of bilayer membrane distortions, there is no clear evidence for periodically perforated membranes. Hence, the eventual perforations should be randomly formed (see Figure 5 and Figure 7S, Supporting Information).

Furthermore, the role of the surfactant component (MO-PEG) not only is to modulate the local curvature changes but also may provoke transient pores in the MO bilayers. The applied temperature stimulus may facilitate the pore enlargement to larger channels in the randomly perforated bilayer. Subsequently, a three-dimensional network of aqueous channels should develop. When a pore opens dynamically with a small size, it could reversibly close (this is the so-called "transient pore"[19a]). The formation of several pores will induce the perforation of the lipid layer (randomly perforated organization) and the transition to a new topology (intermediate) that is detected by large diffuse scattering in the SAXS patterns.

Figure 5 shows a nodal surfaces presentation of the intermediate between a lamellar and a bicontinuous cubic phase. It results from simultaneously occurring events during the soft-matter phase transformation: (i) the PEGylated constituent facilitates the steric distortion of the lipid bilayer. Pores (aqueous channels) form in the distorted bilayer membrane. (ii) Protrusions develop as interlamellar attachments. The generated random single pores and protrusions are shown in Figure 7S of the Supporting Information.

Various terminologies have been advanced to indicate the topological phase transitions passing through intermediate states. The perforations of type (i) have been referred to in the literature[61,62] as fusion pores, funnels, channels, passages, or protrusions. The protuberances of type (ii) have been termed stalks,[61] interlamellar attachments,[12] membrane passages,[62b] diffusive membrane contacts, connecting bridges, interlamellar connections,[62a] or junction zones.[51] Kozlov et al. among other authors[61,62c] have supposed a stalk mechanism of membrane fusion to explain the transient states involving swollen intermediate assemblies. This mechanism includes formation of point contacts, holes, and initial connecting structures between proximal monolayers.

Therefore, the stages in the mechanism of the L → intermediate → cubic D phase transformation could be speculated as: (i) elementary excitations or fluctuations of the bilayer membrane, containing the MO-PEG derivative, leading to the formation of membrane defects such as protrusions and pores (Figure 7S, Supporting Information), (ii) a swollen state, referred to as a long-living intermediate, for which the characteristic spacing of the first peak is q (intermediate) > q (cubic lattice) (Figure 5); (iii) dehydration of the intermediate state and subsequent ordering into a cubic phase upon raising the temperature associated with interfacial curvature increase.

The topological transformations between lamellar and cubic mesophases in lipid and small-amphiphile systems display certain analogy also with the phase transitions in block copolymer assemblies.[54] The intermediate states displaying only a single reflection peak in pressure jump experiments have been considered as *unknown phases*.[47b] Hajduk et al.[39a,b] have reported a hexagonally perforated layer (HPL) morphology as a long-living nonequilibrium state during a lamellar-to-gyroid transition. The gyroid cubic structure has formed upon annealing of this long-living intermediate state.

There is still insufficient proof of how the intermediate states or disrupted phases, which do not display sharp Bragg peaks of a regular periodic structure, topologically look like. The experimental SAXS patterns of long-living metastable transition states have demonstrated the necessity for further theoretical developments. The Lattice Boltzmann model[63] or the self-consistent field method[64] for simulation of nanofluidic compartments in nonperiodic systems present recent perspectives for theoretical advancements in the field.

Conclusion

This structural study was motivated by the necessity to search for sterically stabilized cubosomic drug delivery systems, in which membrane-compatible PEGylated amphiphilic derivatives have major importance. We found that in a system of practical significance (MO/MO-PEG mixture), the lamellar-to-double diamond-cubic phase transition is drastically different in its kinetics and structural features from that in the pure lipid assembly. A sharp epitaxial transition between the lamellar (L) and diamond (D) cubic lattice crystal planes was not observed in the two-component amphiphilic mixture. Intermediate states between L and D phases were stabilized in a broad temperature interval from 1 to 30 °C. The results indicate that the intermediates are present as a long-living metastable phase rather than as millisecond transient structures. These intermediate structures are suggested

(61) (a) Kozlovsky, Y.; Chernomordik, L. V.; Kozlov, M. M. *Biophys. J.* **2002**, *83*, 2634. (b) Yang, L.; Huang, H. W. *Science* **2002**, *297*, 1877–1879. (c) Müller, M.; Katsov, K.; Schick, M. *Phys. Rep.* **2006**, *434*, 113. (d) Efrat, A.; Chernomordik, L. V.; Kozlov, M. M. *Biophys. J. (Biophys. Lett.)* **2007**, L61. (e) Katsov, K.; Müller, M.; Schick, M. *Biophys. J.* **2006**, *90*, 915.

(62) (a) Almgren, M.; Edwards, K.; Karlsson, G. *Colloids Surf. A* **2000**, *174*, 3. (b) Porcar, L.; Hamilton, W. A.; Butler, P. D.; Warr, G. G. *Phys. Rev. Lett.* **2004**, *93*, 198301. (c) Sigel, D. P. *Biophys. J.* **1986**, *49*, 1171.

(63) (a) Nekovee, M.; Coveney, P. V. *J. Am. Chem. Soc.* **2001**, *123*, 12380. (b) González-Segredo, N.; Coveney, P. V. *Phys. Rev. E* **2004**, *69*, 061501. (c) Chen, H.; Kandasamy, S.; Orszag, S.; Shock, R.; Succi, S.; Yakhot, V. *Science* **2003**, *301*, 633–51.

(64) (a) Lee, W. B.; Mezzenga, R.; Fredrickson, G. H. *J. Chem. Phys.* **2008**, *128*, 074504. (b) Lee, W. B.; Mezzenga, R.; Fredrickson, G. H. *Phys. Rev. Lett.* **2007**, *99*, 187801.

to correspond to the growth and ordering of a three-dimensional bicontinuous nanochannel network into a cubic phase.

The SAXS patterns of the intermediate structures obtained with two kinds of amphiphilic systems (MO/MO-PEG and MO/OG) are distinct from a microemulsion phase.[57] They are better fitted with bilayer sponge cell−cell correlations[3b] plus a weakly ordered Pn3m cubic phase. The intermediate state is suggested to be a swollen cubic phase precursor still lacking a long-range crystalline order. It appears to be a general characteristic of the lamellar-to-cubic structural phase transition of the investigated binary amphiphilic mixtures.

Small-angle X-ray and neutron scattering studies of long-living intermediates are essential for understanding of the dynamics of the nanocompartmentalization during the stimuli-induced transformations in self-organized lipid systems. While the melting of the cubic phase to a homogeneous fluid is a rather fast process, the growth of a well-ordered soft-matter cubic structure from sponge-like cubic precursor domains evidently takes extended time.

Acknowledgment. The large scale instrument user support (B.A., A.A.) from DESY (Hamburg, Germany) and LURE (Orsay, France) is gratefully acknowledged. The NMI3 research project has been supported by the European Commission under the 6th Framework Programme through the Key Action: *Strengthening the European Research Area, Research Infrastructures*. Contract n°: RII3-CT-2003-505925. A.A. and B.A. acknowledge continuous cooperation with Dr. C. Bourgaux, Dr. G. Le Bas, and Dr. S.S. Funari. This paper is dedicated to the memory of Dr. M. Ollivon. The authors are indebted to the reviewers for their comments and suggestions.

Supporting Information Available: Additional figures with SAXS patterns and results from simulations. This material is available free of charge via the Internet at http://pubs.acs.org.

LA804225J